Available online at www.sciencedirect.com

ScienceDirect

journal homepage: www.elsevier.com/locate/he

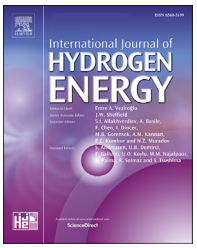

Optimization of powerplant component size on board a fuel cell/battery hybrid bus for fuel economy and system durability

Yongqiang Wang [a], *Scott J. Moura* [b], *Suresh G. Advani* [a], *Ajay K. Prasad* [a,*]

[a] *Center for Fuel Cell and Batteries, Department of Mechanical Engineering, University of Delaware, Newark, DE, 19716, USA*

[b] *Department of Civil and Environmental Engineering, University of California, Berkeley, CA 94720, USA*

ARTICLE INFO

Article history:
Received 6 February 2019
Received in revised form
9 May 2019
Accepted 20 May 2019
Available online xxx

Keywords:
Fuel cell/battery hybrid vehicle
System size
Fuel economy
Durability
Lithium-ion battery

ABSTRACT

The size of the individual powerplant components on board a fuel cell/battery hybrid vehicle affects the power management strategy which determines both the fuel economy and the durability of the fuel cell and the battery, and thus the average lifetime cost of the vehicle. Cost is one of the major barriers to the commercialization of fuel cell vehicles, therefore it is important to study how the sizing configuration affects overall vehicle cost. In this paper, degradation models for the fuel cell and the battery on board a fuel cell/battery hybrid bus are incorporated into the power management system to extend their lifetimes. Different sizing configurations were studied and the results reveal that the optimal size with highest lifetime and lowest average cost is highly dependent on the drive cycle. The vehicle equipped with a small fuel cell stack serving as a range extender will fail earlier and consume more fuel under drive cycles with high average power demand resulting in higher overall cost. However, the same configuration gives optimal results under a standard bus cycle with lower average power demand. At the other end of the spectrum, a fuel cell-dominant bus does not guarantee longer lifetime since the fuel cell operates mostly under low-load conditions which correspond to higher potentials reducing lifetime. Such a configuration also incurs a higher initial capital cost of the fuel cell stack resulting in a high average cost. The best configuration is a battery-dominated system with moderately-sized fuel cell stack which achieves the longest lifetime combined with the lowest average running cost throughout the lifetime of the vehicle.

Introduction

Electric vehicles powered by lithium-ion batteries represent a viable solution to combat climate change caused by the use of fossil fuels in IC engines. Despite progress in lithium-ion battery technology, potential customers are still concerned with its durability, recharging time and especially driving range as compared to IC engines. In contrast, fuel cell vehicles operating on hydrogen offer refueling time and driving range

* *Corresponding author.*
E-mail addresses: sailor@udel.edu (Y. Wang), smoura@berkeley.edu (S.J. Moura), advani@udel.edu (S.G. Advani), prasad@udel.edu (A.K. Prasad).

https://doi.org/10.1016/j.ijhydene.2019.05.160
0360-3199/

comparable to IC engine vehicles. Hence, most major automakers have fuel cell cars in their production portfolio and are poised to release them into the market. Most of these vehicles are quipped with a relatively large fuel cell stack and a small battery. For example, the Toyota Mirai is equipped with a 113 kW fuel cell stack and a 1.6 kWh Nickel-metal hydride battery pack [1]. Such powertrain configurations are intended to let the fuel cell stack provide the majority of the power demand with the battery providing a boost during transient high power-demand situations. On the other hand, fuel cell transit vehicles may employ a small fuel cell stack as a range extender for a large battery pack. The type of configuration will determine the optimal power management strategy which ultimately impacts the fuel economy and durability of the fuel cell stack and battery. For example, two fuel cell hybrid buses with different sized fuel cell stacks were tested in [2] which showed that the bus with a 65 kW fuel cell stack only experienced a 2.4% decrease in performance compared to 10% in the bus with a 100 kW stack due to the wide operating range and high power changing rate of the later stack. Thus, system sizing studies incorporating fuel cell and battery degradation models are required to reduce the average lifetime cost of the hybrid vehicle.

There have been many efforts in the literature to improve the fuel efficiency and lifetime of hybrid vehicles through a sizing study. Methods commonly used include dynamic programming (DP) [3], convex optimization [4], and Pontryagin's minimum principle [5]. The sizing design of a fuel cell hybrid light-duty truck was explored in [3] which concluded that there exists an optimal size with best fuel efficiency. But the resulting power demand on the stack showed rapid fluctuations which are detrimental to stack durability and could significantly shorten its lifetime. The battery sizing study in [6] took fuel cell durability into consideration by adding oxygen excess ratio into the cost function to prevent oxygen starvation which could potentially damage the stack. However, this method is still an indirect attempt to regulate transient power demand on the fuel cell in power management strategies. The sizing study in [4] tried to optimize fuel consumption and cost of the fuel cell stack/battery. A recent paper also considered transient power demand on the fuel cell stack in their optimization algorithm [7]. However, results from both studies [4,7] show that the fuel cell power demand still exhibits rapid variations which exacerbates stress on stack reducing its lifetime. Battery degradation model was included in power management by [8] to find the optimal sizing of plug-in hybrid vehicles with battery and supercapacitors which showed that the operating cost strictly decreases with increasing battery and supercapacitor sizes. The same empirical fuel cell and battery degradation models used in [9] had been considered in the power management system by [10] to study their effects on lifetime cost. Their results showed that the power demand-based control methods are more suitable for vehicles equipped with larger capacity batteries, while the state of charge based control method is better in other cases.

The Center for Fuel Cells and Batteries at the University of Delaware has been conducting a very successful Fuel Cell Bus Program since 2005 to research, build and demonstrate fuel cell-powered buses and hydrogen refueling stations in Delaware [11]. A rule-based power management strategy was proposed to turn on the fuel cell at its optimal efficiency at the appropriate time in the drive cycle based on the predicted energy demand resulting in improved fuel efficiency [12]. The parameters used in this paper are based on the drive cycle data collected from our latest bus (40 ft Gillig platform) equipped with a 58 kW fuel cell stack (three Ballard Mark 9 SSL fuel cell stacks, each rated at 19.4 kW) and a 25 kWh lithium-ion battery (XALT 75 Ah High Power Superior Lithium Ion Cell). The speed profile was extracted to serve as the test drive cycle (UDel drive cycle). The configuration of the vehicle is shown in Fig. 1.

This paper proposes a comprehensive sizing study of a fuel cell hybrid vehicle by considering overall cost including fuel consumption and component durability simultaneously. Degradation models for the fuel cell and battery are directly included in the objective function of the power management system [9]. For fuel cell degradation, a transient power demand constraint is also directly incorporated within the DP optimization framework by treating fuel cell power as a state variable. This method better reflects the operating logic of a real-time power management system and can guarantee a smooth power demand from the stack. This study shows how different sizing configurations would affect the power management strategy and thus the lifetime and the average running cost of the system. The optimal configuration guarantees the best lifetime and lowest average overall cost.

Numerical model

The degradation models of the fuel cell and battery are described in detail in [9]. The fuel cell degradation is modeled by the decrease of electrochemical surface area (ECSA) and the battery degradation by capacity decay. The cost associated with each degradation mechanism is then included in the optimization problem which is solved using DP. The objective

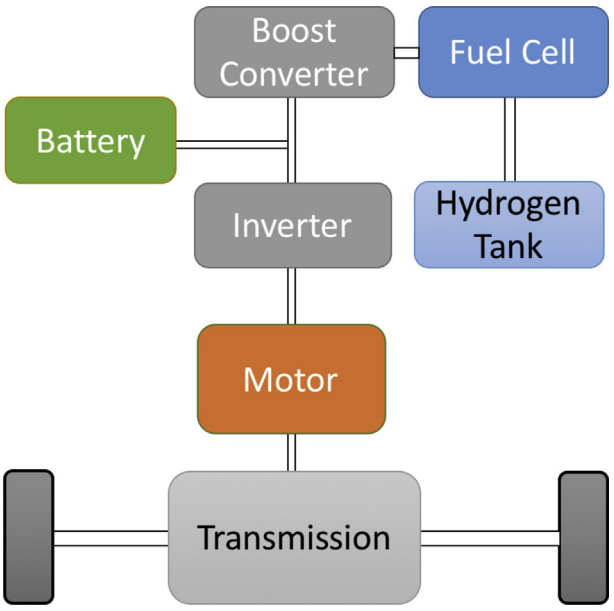

Fig. 1 – The configuration diagram of the hybrid fuel cell bus employed in this study.

Please cite this article as: Wang Y et al., Optimization of powerplant component size on board a fuel cell/battery hybrid bus for fuel economy and system durability, International Journal of Hydrogen Energy, https://doi.org/10.1016/j.ijhydene.2019.05.160

of optimization is to minimize the overall lifetime cost of the hybrid system by minimizing fuel consumption and maximizing fuel cell and battery lifetimes. Hence the objective function is defined as:

$$min \quad J = \int_0^T \left(c_{h_2}\dot{m}_{h_2} + \alpha\left(c_{fc}\dot{A}_{Pt} + c_{pfc}\dot{P}_{fc} + c_{cyl}C + c_{fch}\right) + \beta c_{bat}\dot{B}_{soh}\right)dt$$
$$state: \quad x_k = \left(SoC_k, P_{fc}^{k-1}\right) \tag{1}$$

$$control: \quad u(k) = P_{fc}^{k} \tag{2}$$

$$subject\ to: \quad P_{fc}^{k} \in (P_{min}, P_{max}) \tag{3}$$

$$SoC_k \in (SoC_{min}, SoC_{max}) \tag{4}$$

The two state variables include SoC_k which is the current battery state-of-charge (SoC), and the fuel cell power at the previous timestep P_{fc}^{k-1} which is used to guarantee that the transient power shift does not exceed the maximum fuel cell power ramp rate. The control variable P_{fc}^{k} is directly determined by the optimal state trajectory in this formulation. The hydrogen price c_{h_2} is set to $\$2/kg$ based on DOE's 2020 target for the levelized cost of hydrogen using central water electrolysis [13], and the hydrogen consumption rate is denoted by $\dot{m}_{h_2}$. The fuel cell degradation cost results from several degradation mechanisms: the decay of electrochemical surface area (ECSA) obtained by multiplying the ECSA decay cost c_{fc} by the ECSA decay rate under high potentials $\dot{A}_{Pt}$ which is a function of fuel cell power P_{fc}; the cost due to the transient power load c_{pfc} multiplied by the fuel cell power fluctuation $\dot{P}_{fc}$; the cost due to startup/shutdown cycles c_{cyl} multiplied by the number of such cycles C; and the cost due to high fuel cell power load c_{fch}.

The ECSA decay cost c_{fc} is determined by assuming that an 85% ECSA loss corresponds to the end-of-life (EOL) of the fuel cell stack whose replacement cost is based on DOE's 2020 target of $\$40/kW_{net}$ [14]. The costs due to the other degradation mechanisms are determined as in [15]. The battery decay cost is defined by the state-of-health (SoH) decay rate $\dot{B}_{soh}$ which is a function of C-rate, multiplied by the capital cost to replace the battery c_{bat} which is determined by assuming a total SoH loss at battery EOL using DOE's 2022 target of $\$125/kWh$ [16]. Cost factors α and β are used to scale the costs of the fuel cell stack and battery, respectively, with size; $\alpha = 1$ corresponds to a baseline stack size of 40 kW, and $\beta = 1$ corresponds to a baseline battery size of 11 kWh.

Three drive cycles are considered in this paper. The ECSA loss is calculated by simulating the vehicle's operation under the selected drive cycle for around 1 h which is then scaled up to get the total ECSA loss for longer time periods. Early in life, the ECSA degrades rapidly, hence the scale-up period is kept at 100 h, which is then increased to 500 h in mid-life, and finally to 1000 h towards the end-of-life. A new polarization curve is calculated to account for the ECSA loss after each period and these steps are applied repeatedly until the ECSA declines to 15% of the original value which signifies the end-of-life of the fuel cell stack. The first drive cycle consists of actual data collected during test drives along a chosen route on the University of Delaware campus during which power demand data was also collected. The power demand data was first used to validate a numerical vehicle model as described in [9]. The validated model was then used to calculate the electric power demand for two standard bus drive cycles, namely the Manhattan bus cycle and the Orange County bus cycle. The electric power demand of the traction system can be modeled as:

$$P_{trac} = \left(ma + mg\sin\theta + (C_{r1} + C_{r2}v)mg\cos\theta + \frac{1}{2}\rho A C_d v^2\right)\cdot v / \left(\eta_{trans}\eta_{motor}\eta_{invert}\right) \tag{5}$$

Where m is the mass of the vehicle and a is its acceleration, θ is the road inclination angle ($\theta = \arctan(grade)$), C_{r1} and C_{r2} are rolling resistance coefficients, v is the vehicle velocity, ρ is the air density, A is the vehicle's frontal area, C_d is the aerodynamic drag coefficient, and η_{trans}, η_{motor} and η_{invert} are the efficiencies of the transmission, motor and inverter, respectively. The manufacturer's data shows a relative flat efficiency map for the electric motor across almost all of the operating range. Assuming a fixed efficiency for the transmission and inverter, a combined efficiency around 73% minimized the error between the model and test data. Other model parameters are shown in Table 1.

Results and discussions

This section presents results for the lifetime of the fuel cell stack and the battery under different hybridization configurations to calculate the overall lifetime costs for operating the vehicle. Two battery sizes were selected: 11 kWh which is close to the battery size used by the demonstration fuel cell buses reported by National Renewable Energy Laboratory (NREL) [17], and a smaller 5.5 kWh which represents a fuel cell-dominated hybrid powertrain. It should be noted that the battery capacity on our test bus is much higher (25 kWh) than the ones equipped on commercially-available fuel cell buses due to the lower power density of our batteries. We have chosen to use 5.5–11 kWh in our simulations to be more consistent with what is commercially available at the current time. Since the 11 kWh battery is capable of providing the peak power demand of the electric motor (around 200 kW), larger batteries are not necessary except as range extenders under emergency conditions. The fuel cell size range was selected from 20 kW to 160 kW. 160 kW is similar in size to the stacks used on the demonstration buses reported by NREL, and the

Table 1 – Parameters used in the numerical model of the fuel cell/battery hybrid bus to calculate electric power load under various drive cycles.

Parameters	Values
m	14000 kg
C_{r1}	0.0065
C_{r2}	4.92×10^{-5}
A	$6.5 m^2$
C_d	0.8

Please cite this article as: Wang Y et al., Optimization of powerplant component size on board a fuel cell/battery hybrid bus for fuel economy and system durability, International Journal of Hydrogen Energy, https://doi.org/10.1016/j.ijhydene.2019.05.160

smaller ones are used in the University of Delaware's fuel cell bus fleet. The smaller stacks are considered to explore the optimal hybridization strategy while reducing the total cost.

In the following sections, we first present results for the variation of fuel cell ECSA, battery SOH, and fuel consumption over the entire lifetime of the vehicle, followed by the overall average lifetime costs for all the three drive cycles studied. For the UDel Drive Cycle in particular, we also examine the battery SOC, and fuel cell and battery power profiles over the drive cycle early in the life of the vehicle (after 100 h), followed by the change in the optimal fuel cell power profile over the lifetime of the stack.

Sizing effects under UDel drive cycle

Lifetime and average cost

The fuel consumption and lifetime of the fuel cell and battery with different hybrid configurations are shown in Fig. 2. Fig. 2a shows that the fuel cell ECSA for the 40 kW stack and 11 kWh battery has decayed to 20% of its original value at around 2000 h of operation. Although not at the 15% ECSA threshold designated as stack EOL, the stack had degraded to the extent that it could not provide sufficient net power to achieve the drive cycle, and hence this configuration is deemed to have failed.

Configurations with stacks larger than 40 kW were all able to provide sufficient power to sustain the drive cycle for their entire lifetimes. The 60 kW stack paired with the 11 kWh battery shows the best lifetime of 6883 h while the 80 kW fuel cell with the same battery shows a similar lifetime of 6716 h. Increasing the stack size further reduces its lifetime due to operation at a slightly higher potential at the same power level compared to the smaller stacks. The 120 kW stack's lifetime was 4840 h, while the 160 kW stack's lifetime was further reduced to 4086 h.

As shown in Fig. 2a, the use of a battery smaller than 11 kWh decreases the stack's lifetime dramatically since the stack now needs to provide more of the peak power demand, and must therefore operate under high power for longer durations. Reducing the battery size from 11 kWh to 5.5 kWh reduced the 120 kW stack's lifetime from 4840 to 3633 h (25% reduction), and from 4086 to 3335 h (18% reduction) for the 160 kW stack. Furthermore, the smaller battery fails within the first 1000 h as shown in Fig. 2b because it experiences higher C-rates, whereas the larger battery lasts for around 5000 h.

Fig. 2c shows that smallest stack has a higher fuel consumption rate because it was forced to operate continuously at high power where its efficiency is lower. While the fuel consumption rate is similar for all other stack sizes, the medium-sized 80 kW stack did consume slightly more fuel than the larger stacks due to its lower efficiency under high current draw at similar power loads.

The overall lifetime cost ($/hr) under the UDel Drive Cycle is shown in Fig. 3. The lowest cost of $4.97/hr is obtained with a 80 stack and 11 kWh battery. It should be noticed that although the 60 kW fuel cell stack has the longest lifetime, it does operate in a slightly less efficient regime compared to the 80 kW stack, which results in a slightly higher fuel consumption as shown in Fig. 2c, which consequently increases the lifetime cost. The 40 kW stack results in a 28% increase in

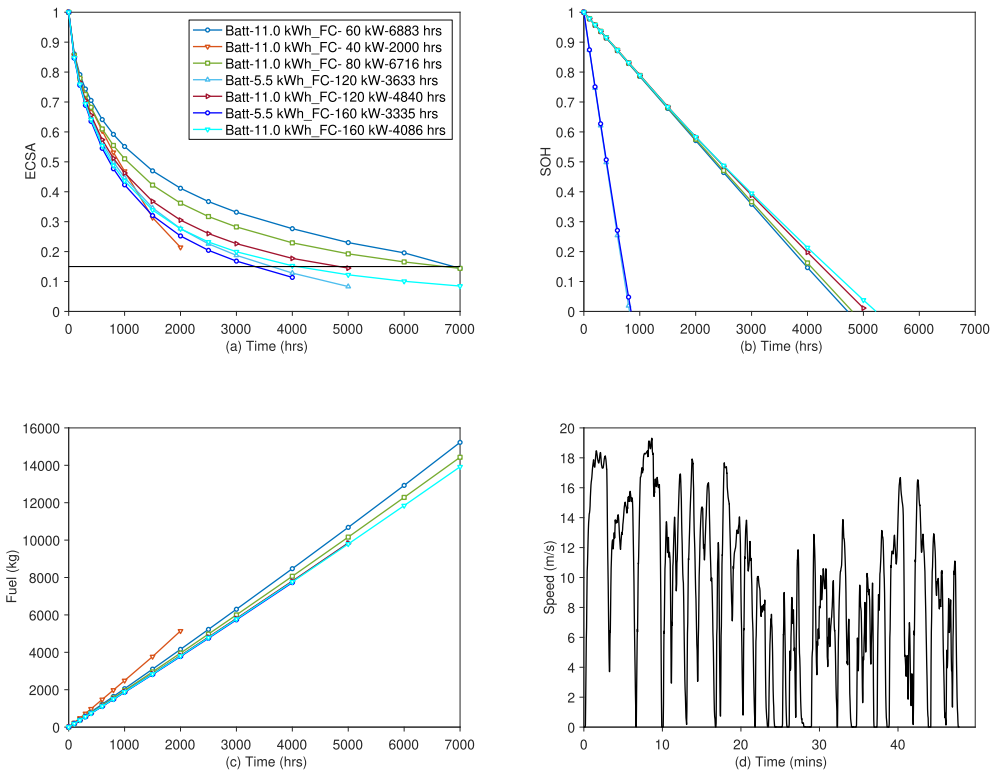

Fig. 2 – Variation of (a) fuel cell ECSA, (b) battery SoH, and (c) fuel consumption over the lifetime of the fuel cell stack under the UDel Drive Cycle which is shown in (d).

Please cite this article as: Wang Y et al., Optimization of powerplant component size on board a fuel cell/battery hybrid bus for fuel economy and system durability, International Journal of Hydrogen Energy, https://doi.org/10.1016/j.ijhydene.2019.05.160

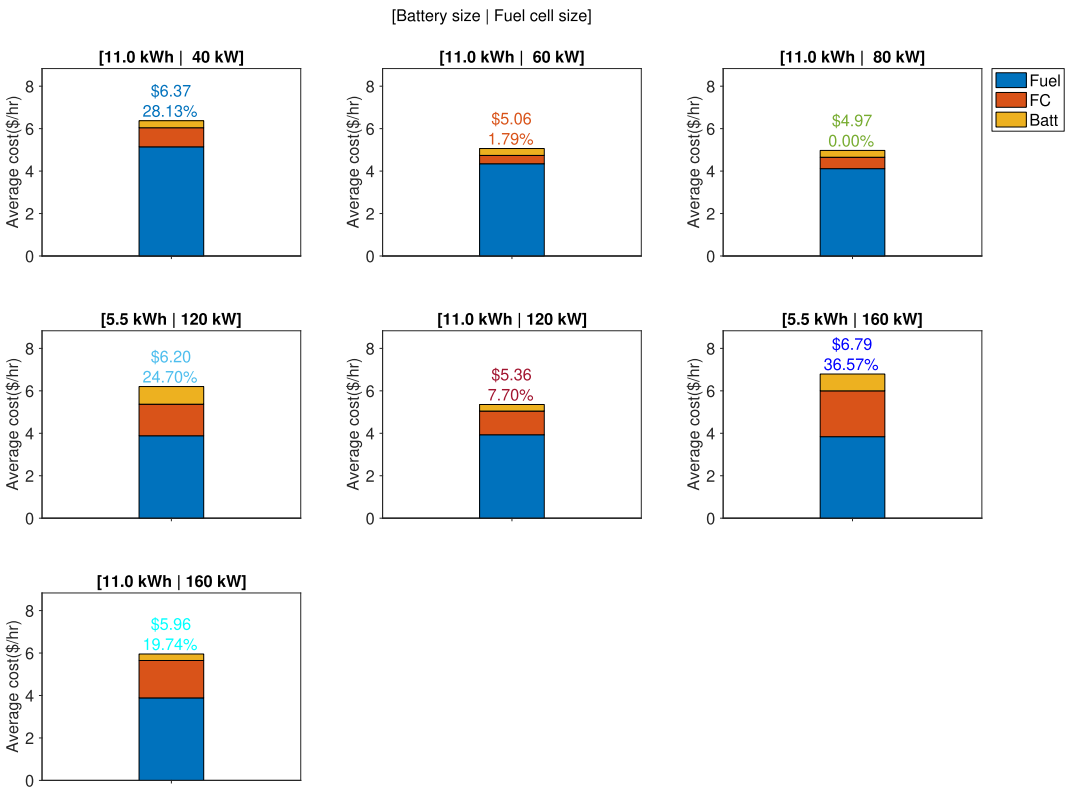

Fig. 3 – Average overall lifetime cost ($/hr) for various fuel cell stack/battery size configurations under the UDel Drive Cycle. The % values indicate cost increases over the optimal case (80 kW stack and 11 kWh battery).

overall costs due to both reduced stack lifetime and higher fuel consumption. Larger stacks show similar fuel consumption compared to the 80 kW stack but the stack costs are much higher due to smaller lifetimes. For the same 11 kW battery, increasing the stack size to 120 kW and 160 kW results in a 7.7% and 19.7% increase in overall cost, respectively.

The two cases with the smaller 5.5 kWh battery show similar stack costs as when paired with the larger battery, but incur a much higher battery cost due shorter lifetimes as a result of higher C-rates. The 5.5 kWh battery paired with a 120 kW and 160 kW stack results in a 24.7% and 36.57% increase in average cost, respectively, compared to the optimal case with a 80 kW stack and 11 kWh battery.

Optimal control strategies

The differences in the resulting lifetimes and average overall costs presented in the previous section can be further explained by analyzing the actual power load on the fuel cell and battery during the drive cycle after 100 h of operation. As shown in Fig. 4, the fuel cell net power loads are mostly maintained around 35 kW due to the high degradation cost associated with stack power fluctuations. The battery net power shows that the battery absorbed most of the transient power demand from the traction system. This means that a smaller battery would suffer a much higher C-rate and capacity decay rate throughout the drive cycle and result in a shorter lifetime as shown in Fig. 2b. The configurations with a 5.5 kWh battery show an elevated fuel cell power output of around 55 kWat the beginning of the drive cycle before dropping back to a lower power subsequently. This is caused by the higher power demand at the beginning of the drive cycle which results in a much higher C-rate for the smaller battery, and thus the power management shifts some of the peak load demand to the stack to balance the degradation between the battery and the stack.

The optimal fuel cell load profiles throughout the lifetime of the fuel cell at different times are shown in Fig. 5. After 2000 h, the fuel cell stack with the smaller battery experiences larger power load fluctuations since the power management begins to divert more transient load away from the battery toward the stack in response to the declining ECSA decay rate. As seen in Fig. 2, the ECSA decays rapidly early in the life of the stack after which the ECSA decay rate decreases significantly. After 4000 h, all fuel cells paired with the 11 kWh battery start to experience some load fluctuations. Unlike the ECSA decay rate, the battery decay rate is constant throughout its decay profile, which prompts the power management to shift more transient load onto the fuel cell to reduce the battery's C-rate, and thus slow down battery decay. After 6000 h, only the configurations with 11 kWh battery and 60 and 80 kW stacks still meet the performance target.

Sizing under standard bus drive cycles

The preceding results pertained to the UDel Drive Cycle which was used to validate our numerical fuel cell bus model. Next, we explore the effect of fuel cell and battery sizing for two standard drive cycles, namely the Manhattan

Please cite this article as: Wang Y et al., Optimization of powerplant component size on board a fuel cell/battery hybrid bus for fuel economy and system durability, International Journal of Hydrogen Energy, https://doi.org/10.1016/j.ijhydene.2019.05.160

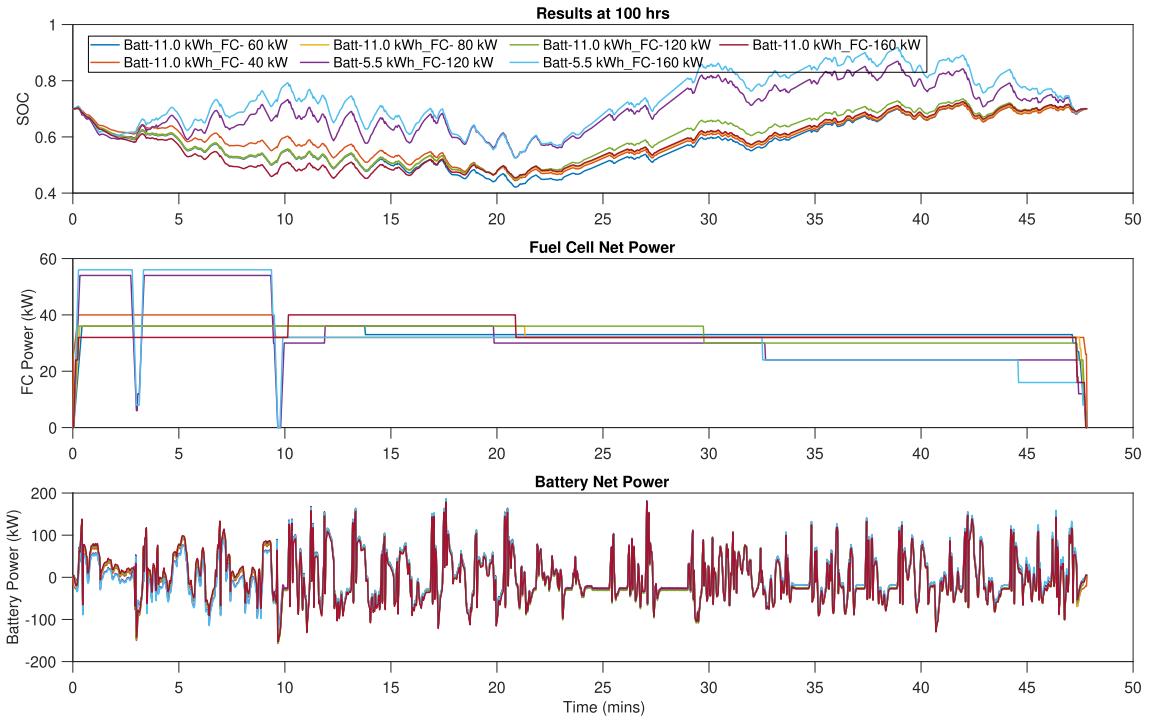

Fig. 4 – Battery SOC, fuel cell net power, and battery net power after 100 h of operation on the UDel Drive Cycle.

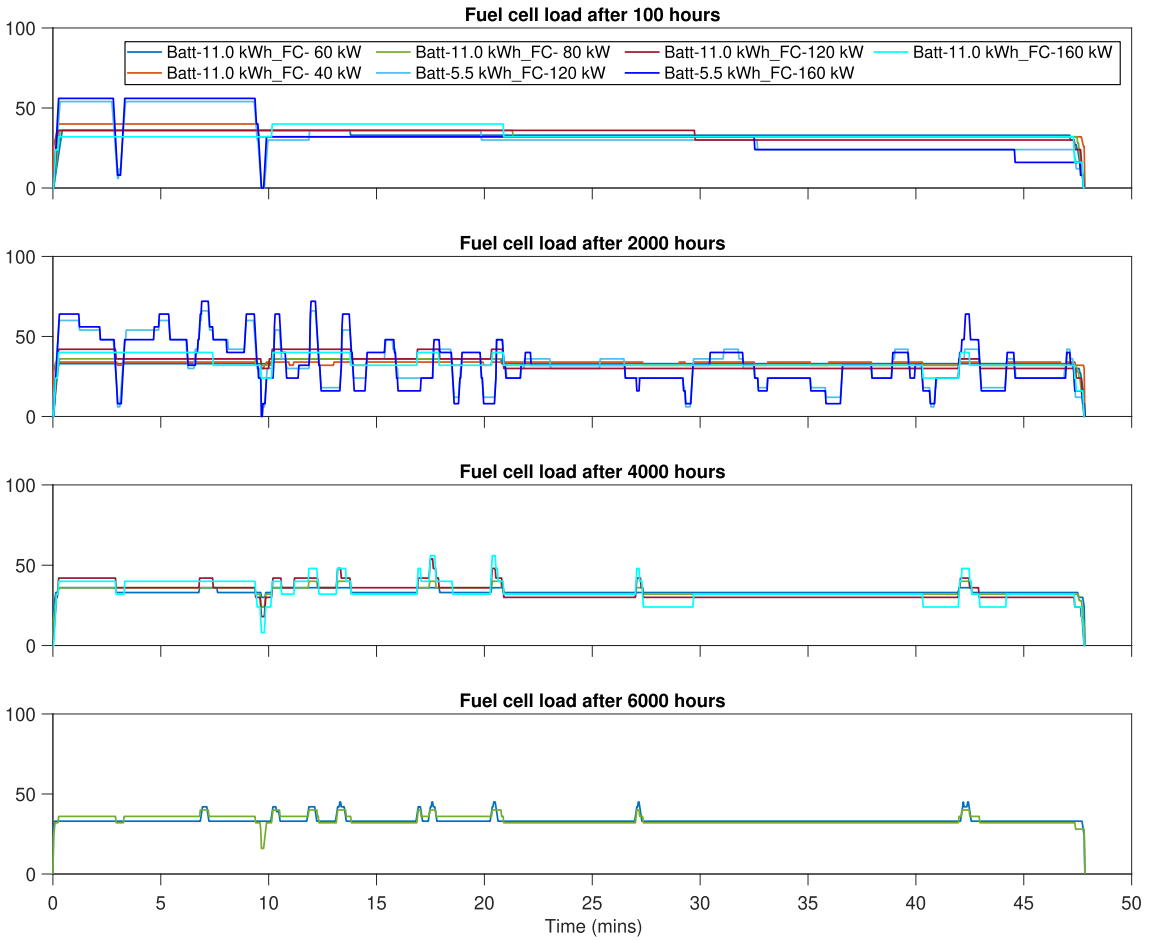

Fig. 5 – Optimal fuel cell load profile (kW) throughout the lifetime of the fuel cell stack as a function of fuel cell and battery size for the UDel Drive Cycle.

Please cite this article as: Wang Y et al., Optimization of powerplant component size on board a fuel cell/battery hybrid bus for fuel economy and system durability, International Journal of Hydrogen Energy, https://doi.org/10.1016/j.ijhydene.2019.05.160

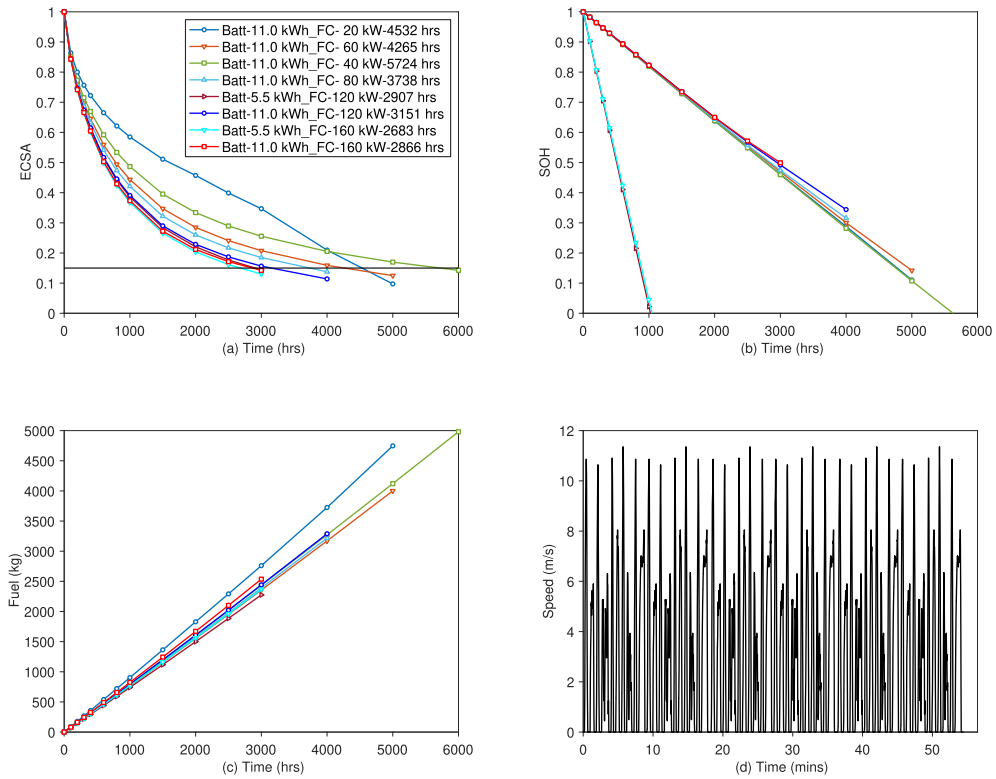

Fig. 6 – Variation of (a) fuel cell ECSA, (b) battery SoH, and (c) fuel consumption over the lifetime of the fuel cell stack under the Manhattan Bus Drive Cycle which is shown in (d).

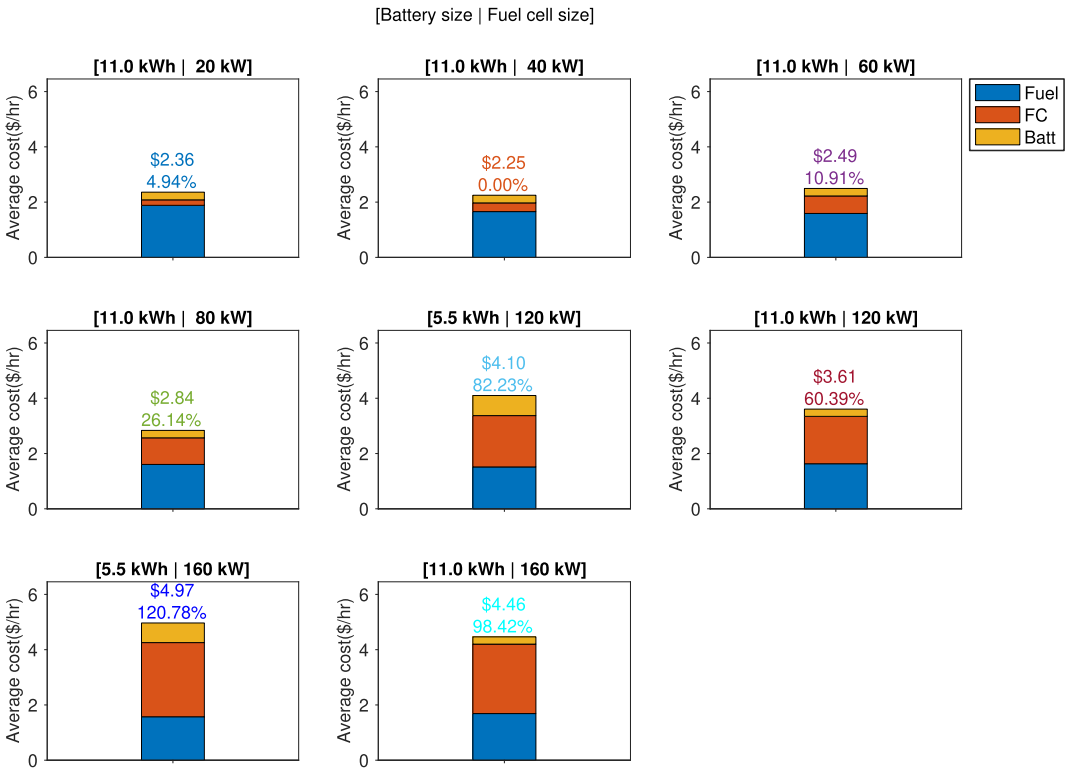

Fig. 7 – Average overall lifetime cost ($/hr) for various fuel cell stack/battery size configurations under the Manhattan Bus Drive Cycle. The % values indicate cost increases over the optimal case (40 kW stack and 11 kWh battery).

Please cite this article as: Wang Y et al., Optimization of powerplant component size on board a fuel cell/battery hybrid bus for fuel economy and system durability, International Journal of Hydrogen Energy, https://doi.org/10.1016/j.ijhydene.2019.05.160

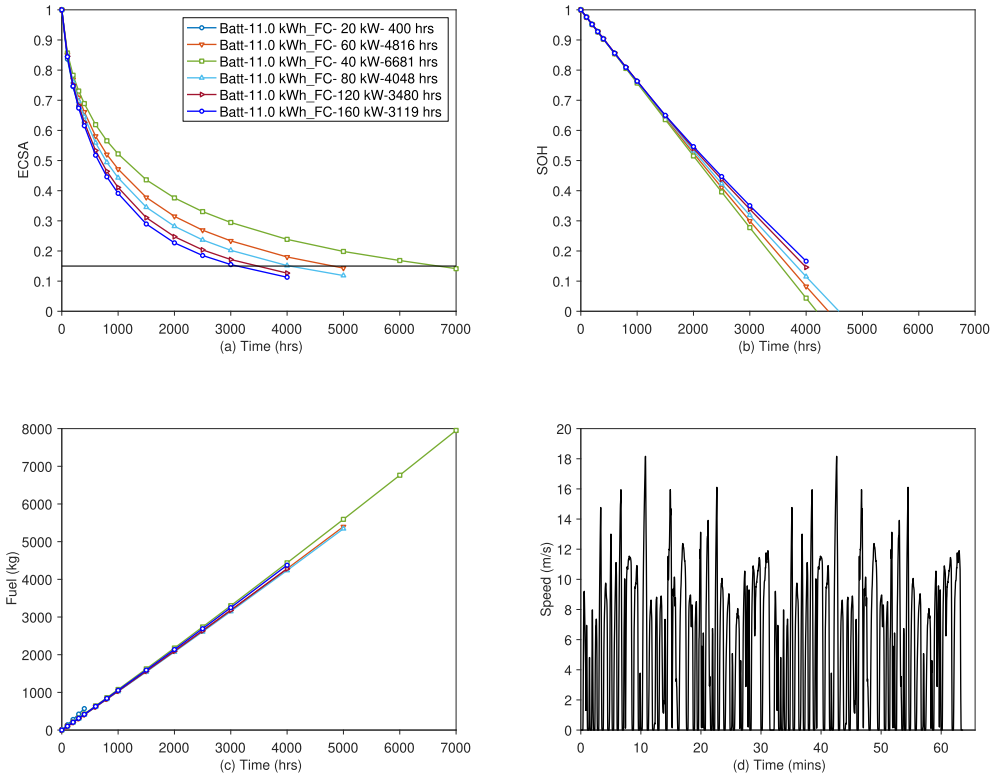

Fig. 8 – Variation of (a) fuel cell ECSA, (b) battery SoH, and (c) fuel consumption over the lifetime of the fuel cell stack under the Orange County Bus Drive Cycle which is shown in (d). (For interpretation of the references to colour in this figure legend, the reader is referred to the Web version of this article).

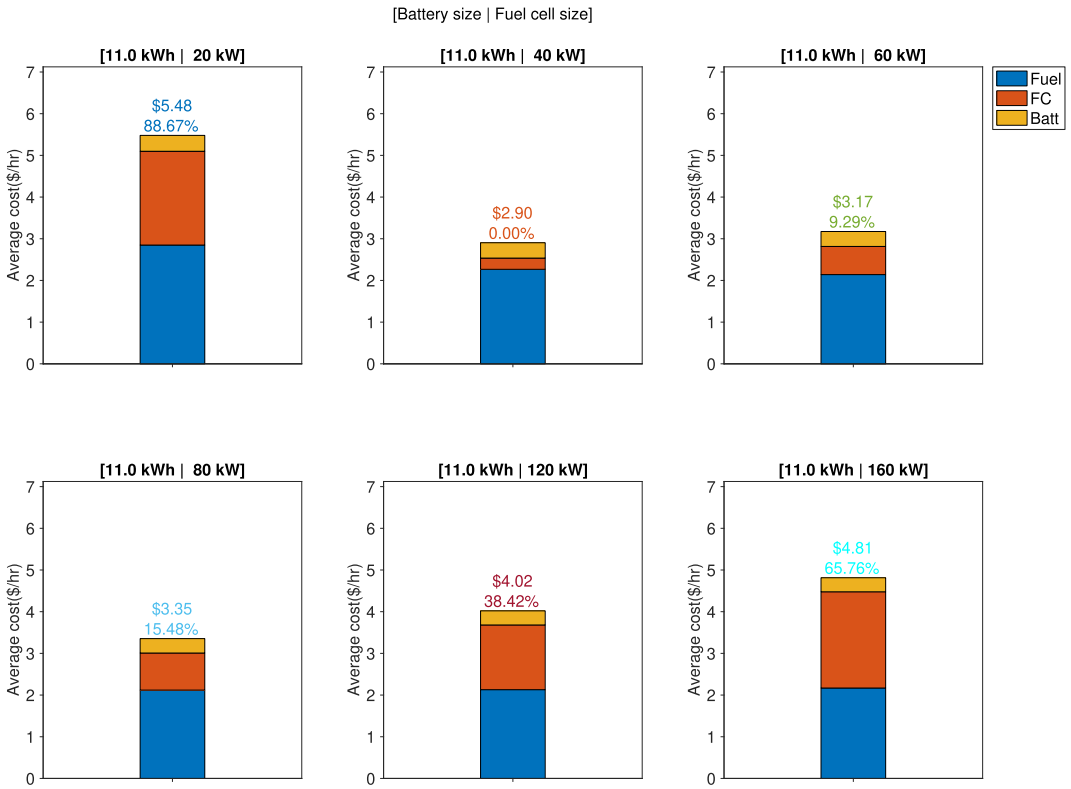

Fig. 9 – Average overall lifetime cost ($/hr) for various fuel cell stack/battery size configurations under the Orange County Bus Drive Cycle. The % values indicate cost increases over the optimal case (40 kW stack and 11 kWh battery). (For interpretation of the references to colour in this figure legend, the reader is referred to the Web version of this article).

Please cite this article as: Wang Y et al., Optimization of powerplant component size on board a fuel cell/battery hybrid bus for fuel economy and system durability, International Journal of Hydrogen Energy, https://doi.org/10.1016/j.ijhydene.2019.05.160

Bus Drive Cycle and Orange County bus Drive Cycle. Of the two, the latter has a slightly higher average speed as it represents an urban/suburban driving scenario. Fig. 6 shows the lifetime of the fuel cell stack, battery SoH decay, and the total fuel consumption of different sizing configurations under the Manhattan Drive Cycle. It can be seen that the 40 kW fuel cell with a 11 kWh battery results in the best lifetime of 5724 h. The case with the 20 kW stack and the same battery shows a slower ECSA decay before 3000 h but thereafter, its decay suddenly accelerates reducing its lifetime only to 4532 h. The reason for this higher decay rate after 3000 h is that the stack operation shifts from a moderate current regime to a high current regime where faster degradation is experienced and thus the ECSA decay accelerates. Other configurations with bigger stacks show similar trends as presented earlier for the UDel Drive Cycle.

The average overall lifetime cost ($/hr) for the Manhattan Bus Drive Cycle is shown in Fig. 7. The optimal configuration consists of a 40 kW fuel cell stack and a 11 kWh battery. The smaller 20 kW fuel cell configuration actually shows a 5% increase in average cost due to its shorter lifetime as explained earlier. The larger stacks show even higher cost increases due to the much higher capital cost of the fuel cells.

The simulation results for the Orange County Drive Cycle are shown in Fig. 8. The results are similar to the Manhattan cycle. The longest lifetime at 6681 h is obtained for the 40 kW stack and 11 kWh battery. This results in the lowest overall average lifetime cost of $2.9/hr as shown in Fig. 9. The results are as expected since both drive cycles have similar average speeds giving similar optimal power management strategies with the fuel cell operating close to the average power demand at all times. The UDel Drive Cycle does not have as many stops as the standard bus drive cycles which results in a much higher average speed and power demand, which yields a larger optimal stack size of 80 kW as discussed in Section Lifetime and average cost.

Conclusions

A comprehensive sizing study of a fuel cell/battery bus was carried out to determine the optimal hybrid configuration accounting for the degradation experienced both by the fuel cell stack and the battery over the vehicle's lifetime. It is shown that a configuration consisting of a small fuel cell stack whose power just exceeds the average vehicle power demand over the drive cycle will degrade rapidly due to the high current draw and experience premature failure. On the other hand, a fuel cell-dominated configuration with a small battery would place excessive transient power demand on the stack reducing its lifetime, which combined with its higher initial capital cost, would further increase the overall lifetime cost. In contrast, a battery-dominated system would extend stack life since the battery absorbs most of the transient power demand. It is shown that a battery-dominated configuration with the battery providing peak traction power paired with a moderate-sized fuel cell stack maximizes stack lifetime and results in the lowest overall average lifetime cost. It is also shown that the optimal size is greatly influenced by the average power demand of specific drive cycles, which means that the same bus operating on drive cycles with different characteristics (starts and stops, average speed, terrain, etc.) could experience significant cost differences. Thus, it is prudent to match the hybrid configuration to the actual drive cycle to reduce the vehicle's overall lifetime cost. In reality, this is possible since most transit buses operate on only one or a few fixed routes throughout their lifetime.

Acknowledgment

This work was conducted under the University of Delaware's Fuel Cell Bus Program to research, build, and demonstrate fuel cell powered hybrid vehicles for transit applications. This program is funded by the Federal Transit Administration. Partial funding for this work was also provided by the Mid-Atlantic Transportation Sustainability University Transportation Center.

REFERENCES

[1] Wikipedia. Toyota Mirai — wikipedia, the free encyclopedia. 2016. Online; accessed 1-July-2016, https://en.wikipedia.org/w/index.php?title=Toyota_Mirai&oldid=726813544.

[2] Ouyang M, Xu L, Li J, Lu L, Gao D, Xie Q. Performance comparison of two fuel cell hybrid buses with different powertrain and energy management strategies. J Power Sources 2006;163(1):467–79. special issue including selected papers presented at the Second International Conference on Polymer Batteries and Fuel Cells together with regular papers, https://doi.org/10.1016/j.jpowsour.2006.09.033. http://www.sciencedirect.com/science/article/pii/S0378775306019367.

[3] Tazelaar E, Shen Y, Veenhuizen PA, Hofman T, van den Bosch PPJ. Sizing stack and battery of a fuel cell hybrid distribution truck. Oil Gas Sci Technol Rev IFP Energies nouvelles 2012;67(4):563–73. https://doi.org/10.2516/ogst/2012014. https://doi.org/10.2516/ogst/2012014.

[4] Hu X, Murgovski N, Johannesson LM, Egardt B. Optimal dimensioning and power management of a fuel cell battery hybrid bus via convex programming. IEEE ASME Trans Mechatron 2015;20(1):457–68. https://doi.org/10.1109/TMECH.2014.2336264.

[5] Liu C, Liu L. Optimal power source sizing of fuel cell hybrid vehicles based on Pontryagin's minimum principle. Int J Hydrogen Energy 2015;40(26):8454–64. https://doi.org/10.1016/j.ijhydene.2015.04.112. http://www.sciencedirect.com/science/article/pii/S0360319915010241.

[6] Sundström O, Stefanopoulou A. Optimum battery size for fuel cell hybrid electric vehicle with transient loading consideration—part ii. J Fuel Cell Sci Technol 2006;4(2):176–84. https://doi.org/10.1115/1.2713779.

[7] Hu X, Jiang J, Egardt B, Cao D. Advanced power-source integration in hybrid electric vehicles: multicriteria optimization approach. IEEE Trans Ind Electron 2015;62(12):7847–58. https://doi.org/10.1109/TIE.2015.2463770.

[8] Song Z, Zhang X, Li J, Hofmann H, Ouyang M, Du J. Component sizing optimization of plug-in hybrid electric vehicles with the hybrid energy storage system. Energy 2018;144:393–403. https://doi.org/10.1016/j.energy.2017.12.009. http://www.sciencedirect.com/science/article/pii/S0360544217320285.

[9] Wang Y, Moura SJ, Advani SG, Prasad AK. Power management system for a fuel cell/battery hybrid vehicle incorporating fuel cell and battery degradation. Int J Hydrogen Energy 2019;44(16):8479–92. https://doi.org/10.1016/j.ijhydene.2019.02.003. http://www.sciencedirect.com/science/article/pii/S0360319919305014.
[10] Hu Z, Li J, Xu L, Song Z, Fang C, Ouyang M, Dou G, Kou G. Multi-objective energy management optimization and parameter sizing for proton exchange membrane hybrid fuel cell vehicles. Energy Convers Manag 2016;129:108–21. https://doi.org/10.1016/j.enconman.2016.09.082. http://www.sciencedirect.com/science/article/pii/S0196890416308871.
[11] Bubna P, Brunner D, Gangloff Jr JJ, Advani SG, Prasad AK. Analysis, operation and maintenance of a fuel cell/battery series-hybrid bus for urban transit applications. J Power Sources 2010;195(12):3939–49. https://doi.org/10.1016/j.jpowsour.2009.12.080. http://www.sciencedirect.com/science/article/pii/S0378775309023428.
[12] Bubna P, Brunner D, Advani SG, Prasad AK. Prediction-based optimal power management in a fuel cell/battery plug-in hybrid vehicle. J Power Sources 2010;195(19):6699–708. https://doi.org/10.1016/j.jpowsour.2010.04.008. http://www.sciencedirect.com/science/article/pii/S0378775310005896.
[13] DOE. DOE technical targets for hydrogen production from electrolysis. 2011. https://www.energy.gov/eere/fuelcells/doe-technical-targets-hydrogen-production-electrolysis.
[14] DOE. DOE technical targets for fuel cell systems and stacks for transportation applications. 2015. https://energy.gov/eere/fuelcells/doe-technical-targets-fuel-cell-systems-and-stacks-transportation-applications.
[15] Pei P, Chang Q, Tang T. A quick evaluating method for automotive fuel cell lifetime. Int J Hydrogen Energy 2008;33(14):3829–36. tMS07: Symposium on Materials in Clean Power Systems, https://doi.org/10.1016/j.ijhydene.2008.04.048. http://www.sciencedirect.com/science/article/pii/S036031990800476X.
[16] DOE. Overview of the DOE VTO advanced battery RD program. 2016. https://energy.gov/sites/prod/files/2016/06/f32/es000_howell_2016_o_web.pdf.
[17] NREL. Fuel cell buses in u.s. transit fleets: current status 2017. 2017. https://www.osti.gov/biblio/1410409.

Please cite this article as: Wang Y et al., Optimization of powerplant component size on board a fuel cell/battery hybrid bus for fuel economy and system durability, International Journal of Hydrogen Energy, https://doi.org/10.1016/j.ijhydene.2019.05.160